

Simulating Ground Thermal Anomaly under Conditions of Dense Vegetation Based On Lab and Field Measurements to Support Thermal Infrared Remote Sensing Techniques

Asep Saepuloh¹, Suryantini¹, Christoph Hecker², Robert Hewson²

¹Faculty of Earth Sciences and Technology, Institut Teknologi Bandung, Bandung, Indonesia

²Faculty of ITC, University of Twente, Twente, The Netherlands
saepuloh@gc.itb.ac.id

Keywords: Land Surface Temperature, Geothermal, FLIR C2, kinetic temperature, vegetation

ABSTRACT

The ground temperature and emissivity anomalies could be used as an indicator for the existence of geothermal surface manifestations such as hot springs, fumaroles, or altered surfaces with remaining thermal at a crater rim. The ground temperature could be measured directly at the field using ground thermometer. However, field measurements are inefficient for large investigated areas and extracting Land Surface Temperature (LST) based on satellite thermal infrared sensor is also complicated due to several unknown parameters such as noise from the environment and object emissivity. Moreover, field studies under the conditions of dense vegetation makes the problem worse due to the shallower layer penetration of the response at wavelengths of thermal infrared compared to microwave energies. Overcoming the problem, we tried to estimate the kinetic temperature from the simulated steam spot using thermal infrared camera FLIR C2 with an accuracy of 2°C. The lab simulations were performed proportionally to ground variables such as the vegetation cover, height of the sensor, and diurnal effects. According to the simulations, the steam spot from boiling water 98°C recorded by the sensor at heights more than 1.2 m equivalent to spatial resolution 0.2 cm is constant about 37.2°C. We also observed that the vegetation cover reduced the measured temperature with thermal efficiency 33%. For diurnal effect, the detected temperature is constant regardless time observations. The background temperature influenced the vegetation covering steam spot with efficiencies 30% and 50% for day and night observations, respectively. These simulation results were used for further study into thermal infrared remote sensing techniques for thermal features identification. Field investigations were also performed to clarify the applicability of the thermal infrared camera to the measured ground temperature.

1. Introduction

The temperature and emissivity anomalies extracted from thermal infrared (TIR) remote sensing could be used as an indicator for the existence of geothermal surface manifestations such as hot springs, fumaroles, mud pools, and steaming ground (Hodder, 1970). The ground temperature could be measured directly at the field using contact system such as ground thermometer. However, field measurements are inefficient for large investigated areas (Saepuloh et al., 2013). The laboratory and field experiments presented in this paper are aimed to support thermal infrared remote sensing for geothermal features detection (Kuenzer and Dech, 2013).

Extracting kinetic temperature of ground target based on satellite thermal infrared is complicated due to several unknown parameters such as emissivity and noise from environment (Kahle and Alley, 1992). Therefore, brightness temperature is the most optimal applicable parameter to assess the ground thermal anomaly in assumption that the atmospheric effect is not significant (Jiménez-Muñoz and

Sobrino, 2003). Moreover, investigated field study under conditions of dense vegetation makes the problem worse due to the shallower layer penetration of the response at wavelengths of thermal infrared compared to microwave energies (Saepuloh et al., 2012).

In this study we simulated the “steam spots” as detected by the thermal infrared camera using a boiling water to obtain the effect of sensor height and variation of vegetation cover as well as diurnal temperature to the measured steam spot. We also calculated the effect of resolution to the measured temperature and efficiency of vegetation covers reducing temperature of targets. In addition to the lab measurement, we also measured ground temperature at mud pool, steaming ground (altered surface), and hot spring using the same thermal infrared camera.

2. Equipment and method

Detecting kinetic temperature of the objects at ground surface level is the aim of the thermal infrared remote sensing. Straight forward to the problem, we applied a simulation to estimate the kinetic temperature from a steam spot using thermal infrared camera FLIR C2. The FLIR C2 is a pocket-sized thermal camera and designed for a wide range of applications to find heat patterns that point out hotspots. The camera was utilized by visible (VIS) and infrared (IR) sensors with spectral range 7.5 - 14 μm and resolution 640×480 pixels for VIS and 80×60 pixels for IR sensor (FLIR, 2014). The object temperature range -10°C to 150°C with accuracy ±2°C makes this camera is plausible for measurement at geothermal field.

Measuring the target temperature, a static 200 cm vertical road was used as center of the height adjustable camera positions. Then, the steam spot was simulated using boiling water which is maintained temperature at 98°C by a heater pot and located at the bottom part of the vertical road (Figure 1). The lab simulations were performed proportional to ground variables including height of the sensor, vegetation cover, and diurnal effect. To obtain the elevation and the resolution impact to the measured temperature, the steam spot was measured every 5 cm height. The minimum and maximum heights are located at the pot cover (=0 cm) and top of the road (=200 cm), respectively. According to this method, the camera produced 40 measurements from different height. For analyzing vegetation cover to the measured temperature, we used leaves cover 0, 25, 50, 75, and 100% of total upper pot surface area. Cover 0 and 100% mean that the upper pot are opened and closed totally by vegetation, respectively. This experiment will support the evidence of temperature relationship for partial canopy cover conditions (Kustas and Anderson, 2009). To obtain the air temperature variation over time to the measured temperature, we measured the steam spot every hour in open area for 24 hours. The measurements were performed using fixed height 200 cm and vegetation cover 0 and 25%.



Figure 1. Experimental design using FLIR C2 at lab scale to measure a simulated steam spot using boiling water.

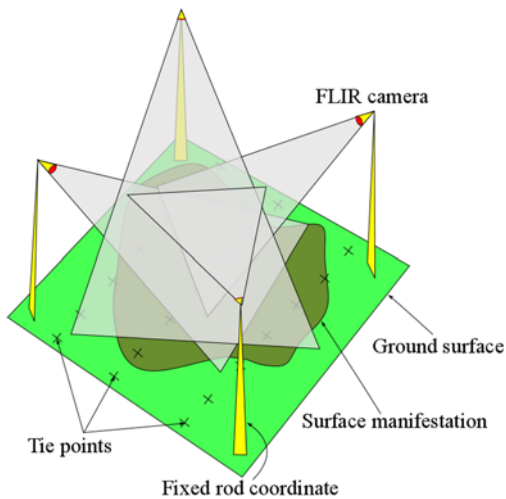


Figure 2. Surface temperature measurement design at field using FLIR C2 camera.

Confirming the applicability of the thermal infrared camera and lab measurement results, we also performed a field scale measurement using the same thermal infrared camera. The field measurements were designed following 1 m grid scanning for each surface thermal feature illustrated by dark green zone in Figure 2. The height of camera was fixed 200 cm to keep a constant spatial resolution. There were three measured locations of surface thermal features consisting mud pool, steaming ground, and hot spring at Wayang Windu Geothermal Field. The number of grid at each location was selected according to terrain and safety conditions.

3. Lab scale experimental results

The first experiment is aimed to obtain the sensor elevation sensitivity to the measured temperature. The steam spot measurements were performed indoor with room temperature 25.5°C at 13.40 AM. The thermal infrared camera was aimed to the target vertically and the boiling water inside the pot was opened to the free air. The measured temperatures with height variation were depicted in Figure 3A. There is no clear correlation due to large different temperature variation within height. However, the general trend is a decreasing temperature along with increasing sensor height. The large variation of measured temperature presented by medium correlation determination (R^2) about 0.5 was predicted by contact of the water vapor to the sensor. An opened water pot caused a contact between the water vapor and the lens of the sensor. Therefore, the measured temperature is higher and lower than the steam spot itself.

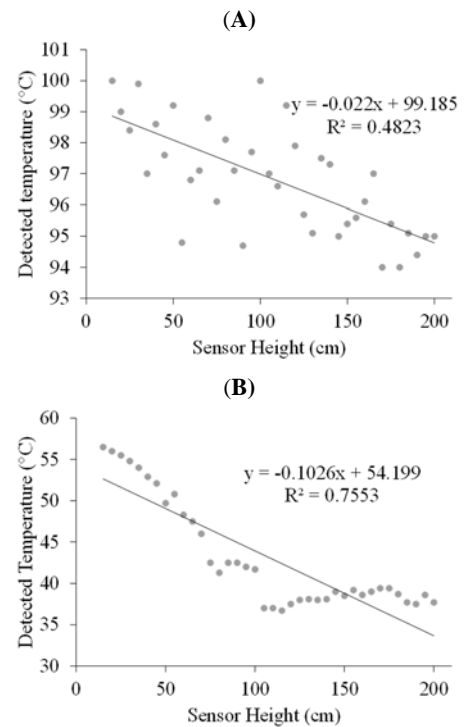


Figure 3. Large variation of detected temperature at different sensor height due to water vapor effect (A) and small variation from isolated steam spot with constant temperature achieved at height more than 120 cm (B).

Omitting the contact with water vapor, we used a closed water pot so that the measured target is the heated cap of the water pot. A relatively persistent decreasing curve was obtained by this method as presented by Figure 3B. The decreasing curve pattern was consistent up to sensor height 120 cm. The higher sensor position than 120 cm showed that the measured temperature is constant about 37.2°C. The lower variation of measured temperature presented by higher R^2 about 0.8 than opened pot was achieved.

The second experiment was a vegetation cover effect to the measured temperatures by the sensor. The result showed that the decreasing temperatures agreed with the increase of vegetation covers (Figure 4A). The high R^2 about 0.98 indicated that vegetation cover affected the measured temperature persistently. According to the measurement, a small thermal signature could be detected at 100% vegetation cover with thermal efficiency 0.33 ($=31^\circ\text{C}/94.48^\circ\text{C}$). This condition encourages the usability of thermal infrared sensor even though under dense vegetation cover.

For the third condition, the experiment is aimed to obtain the background temperature from the diurnal effect. The fixed sensor height at 200 cm was used under two conditions of vegetation cover: 0 and 25%. The measurement results are depicted by Figure 4B. The air temperatures which were measured every hour showed almost constant about 27°C. For vegetation cover 0%, the measured steam spot temperatures are also almost constant regardless time observation about 98°C. On the contrary, the large variation of measured temperatures was obtained under vegetation covers 25%. According to the 2nd experiment, the measured temperatures should be constant about 80°C. The large temperature variation under vegetation 25% infers that the vegetation covers affected strongly by diurnal temperature, but not for the steam spot.

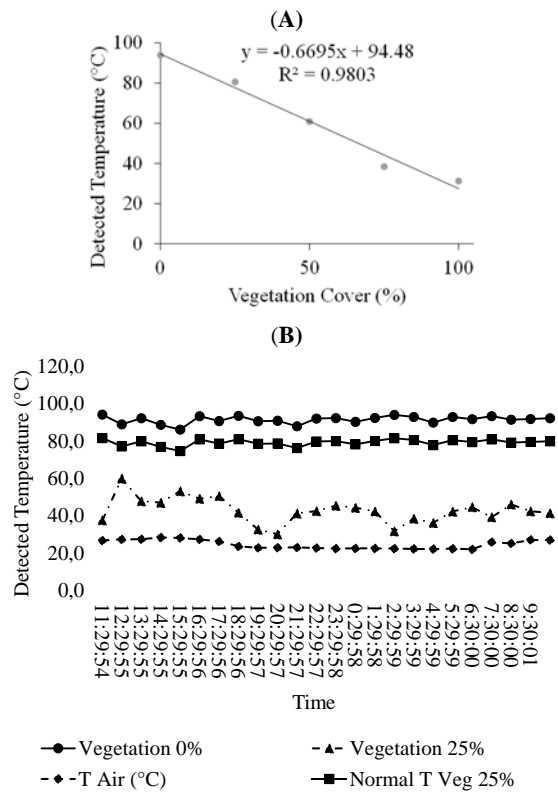


Figure 4. Vegetation reduces detected temperature gradually, but small signature still observed at 100% covers with thermal efficiency 0.33 (A) and the steam spot temperature is constant over time and independently to diurnal temperature (B).

4. Field scale experimental results

Obtaining the applicability of the thermal camera for field measurement, we measured three locations of surface thermal features. The first feature was located at mud pool presented by Figure 5A. The ground surface at this location is covered by thick vegetation presented by green portions in the aerial photographs.

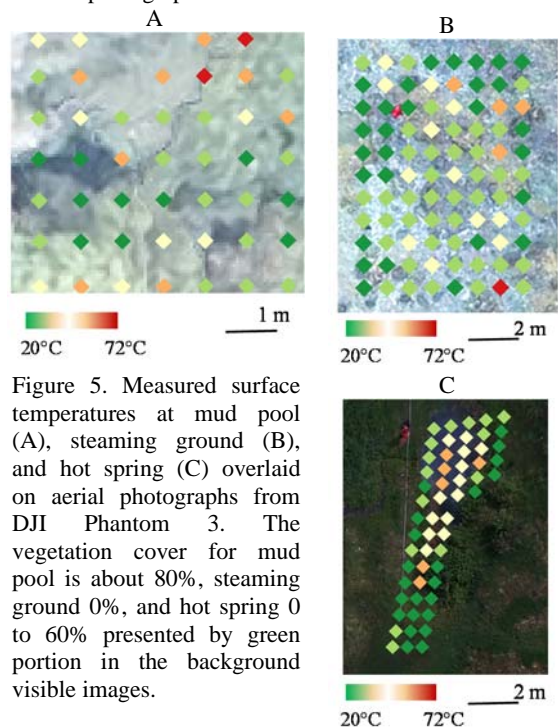


Figure 5. Measured surface temperatures at mud pool (A), steaming ground (B), and hot spring (C) overlaid on aerial photographs from DJI Phantom 3. The vegetation cover for mud pool is about 80%, steaming ground 0%, and hot spring 0 to 60% presented by green portion in the background visible images.

There were about 80% ground surface covered by grasses and trees. Therefore, the satellite thermal infrared sensor will detect only small amount of the remaining surface temperature. According to the 2nd lab measurement, the thermal efficiency for 80% vegetation cover is 0.43. Therefore, the ground temperature about 72°C might be detected by the thermal infrared sensor about 29.5°C.

On the contrary, there are no vegetation covers at steaming ground presented by Figure 5B. The ground surfaces are composed chiefly by alteration clays and fumaroles. Some spots contained ground thermal presented by high temperature more than 60°C on the bright spots of the aerial photographs. For the hot spring, the maximum detected temperature is about 53°C at the hot water surfaces. Some spots at the ground surfaces covered by grass were also detected higher than surrounding temperatures. The green pale of the grass in the aerial photographs was predicted as stressed vegetation due to soil contact with hydrothermal fluid.

5. Conclusion

The height of sensor reduced the detected temperature, but constant measurement was achieved at height more than 120 cm. Decreasing detected temperature is concordance with sensor resolution, but constant at low image resolution less than 0.2 cm. Vegetation also reduces the detected temperature constantly, but small signature still observed at 100% cover with thermal efficiency 0.33. The target temperature is constant over time and independently to the background temperature. The vegetation reduced temperature about 30% in the day and 50% in the night observations. The presented experimental results will be used for correcting ground temperature derived by TIR remote sensing.

References

- FLIR, 2014. User's manual FLIR Cx series.
- Hodder, D.T., 1970. Application of remote sensing to geothermal prospecting. *Geothermics* 2, 368IN1369-380.
- Jiménez-Muñoz, J.C., Sobrino, J.A., 2003. A generalized single-channel method for retrieving land surface temperature from remote sensing data. *J. Geophys. Res. Atmospheres* 108.
- Kahle, A.B., Alley, R.E., 1992. Separation of temperature and emittance in remotely sensed radiance measurements. *Remote Sens. Environ.* 42, 107–111.
- Kuenzer, C., Dech, S., 2013. Thermal infrared remote sensing. *Sens. Methods Appl. Remote Sens. Digit. Image Process.* 17.
- Kustas, W., Anderson, M., 2009. Advances in thermal infrared remote sensing for land surface modeling. *Agric. For. Meteorol.* 149, 2071–2081.
- Saepuloh, A., Koike, K., Omura, M., 2012. Applying Bayesian Decision Classification to Pi-SAR polarimetric data for detailed extraction of the geomorphologic and structural features of an active volcano. *IEEE Geosci. Remote Sens. Lett.* 9, 554–558.
- Saepuloh, A., Urai, M., Aisyah, N., Sunarta, Widiwijayanti, C., Subandriyo, Jousset, P., 2013. Interpretation of ground surface changes prior to the 2010 large eruption of Merapi volcano using ALOS/PALSAR, ASTER TIR and gas emission data. *J. Volcanol. Geotherm. Res., Merapi eruption* 261, 130–143.